Acta Crystallographica Section F
Structural Biology and Crystallization Communications
ISSN 1744-3091

D. C. Bensen, S. Rodriguez, J. Nix, M. L. Cunningham and L. W. Tari*

Structural Biology, Trius Therapeutics, 6310 Nancy Ridge Drive, Suite 101, San Diego, CA 92008, USA

Correspondence e-mail: ltari@triusrx.com

Received 28 January 2012
Accepted 14 February 2012

PDB Reference: MurA–UNAG–fosfomycin complex, 3vcy.

Structure of MurA (UDP-*N*-acetylglucosamine enolpyruvyl transferase) from *Vibrio fischeri* in complex with substrate UDP-*N*-acetylglucosamine and the drug fosfomycin

The development of new antibiotics is necessitated by the rapid development of resistance to current therapies. UDP-*N*-acetylglucosamine enolpyruvyl transferase (MurA), which catalyzes the first committed step of bacterial peptidoglycan biosynthesis, is a prime candidate for therapeutic intervention. MurA is the target of the antibiotic fosfomycin, a natural product produced by *Streptomyces*. Despite possessing a high degree of sequence conservation with MurA enzymes from fosfomycin-susceptible organisms, recent microbiological studies suggest that MurA from *Vibrio fischeri* (VfiMurA) may confer fosfomycin resistance *via* a mechanism that is not yet understood. The crystal structure of VfiMurA in a ternary complex with the substrate UDP-*N*-acetylglucosamine (UNAG) and fosfomycin has been solved to a resolution of 1.93 Å. Fosfomycin is known to inhibit MurA by covalently binding to a highly conserved cysteine in the active site of the enzyme. A comparison of the title structure with the structure of fosfomycin-susceptible *Haemophilus influenzae* MurA (PDB entry 2rl2) revealed strikingly similar conformations of the mobile substrate-binding loop and clear electron density for a fosfomycin–cysteine adduct. Based on these results, there are no distinguishing sequence/structural features in VfiMurA that would translate to a diminished sensitivity to fosfomycin. However, VfiMurA is a robust crystallizer and shares high sequence identity with many clinically relevant bacterial pathogens. Thus, it would serve as an ideal system for use in the structure-guided optimization of new antibacterial agents.

1. Introduction

Peptidoglycan is the major structural component of the cell wall in Gram-positive and Gram-negative bacteria. Peptidoglycan is a macromolecule consisting of long amino-sugar strands cross-linked by short (three-amino-acid to five-amino-acid) polypeptide chains. UDP-*N*-acetylglucosamine enolpyruvyl transferase (MurA) catalyzes the first committed step in peptidoglycan biosynthesis by transferring enolpyruvate from phosphoenol pyruvate (PEP) to UDP-*N*-acetylglucosamine (UNAG) to form enolpyruvyl-UDP-*N*-acetylglucosamine (EP-UNAG) (Bugg & Walsh, 1992). MurA is an ideal target for the design of new classes of antibacterial inhibitors; it is highly conserved across both Gram-positive and Gram-negative bacteria, is essential for cell survival and has no human homolog. Furthermore, it is the target of the natural product antimicrobial agent fosfomycin (Kahan *et al.*, 1974).

The inhibition of MurA by fosfomycin has been extensively characterized both structurally and biochemically (Walsh *et al.*, 1996). Fosfomycin is a PEP mimetic that acts by alkylating the highly conserved Cys115 (*Escherichia coli* numbering) of MurA (Kahan *et al.*, 1974). Previous crystal structures have shown that Cys115 is located on a highly mobile loop which has been observed to adopt one of three different conformations (Yoon *et al.*, 2008). The open-loop conformation, such as in the unliganded MurA from *Entero bacter cloacae* (Schönbrunn *et al.*, 1996), is contrasted by the closed-loop ternary structure of *E. coli* MurA, which places the Cys–fosfomycin deep in the active site (Skarzynski *et al.*, 1996). Another

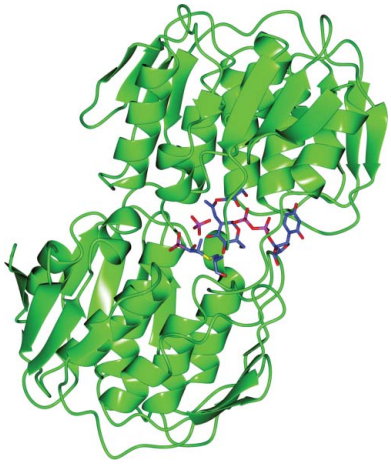

form, which places the loop in a half-open conformation, has been observed in both the binary and ternary structures of *Haemophilus influenzae* MurA (Yoon *et al.*, 2008).

Resistance mechanisms to fosfomycin are varied. In the bacterial pathogens *Mycobacterium tuberculosis* and *Chlamydia trachomatis*, an active-site cysteine-to-aspartate substitution accounts for naturally occurring insensitivity (De Smet *et al.*, 1999; McCoy *et al.*, 2003). Enzymatic modification of fosfomycin by the widely distributed enzymes FosA, FosB and FosX acts by opening the epoxide ring, thus rendering the drug ineffective (Rigsby *et al.*, 2005; Fillgrove *et al.*, 2003). Recently, MurA from the marine Gram-negative bacterium *Vibrio fischeri* has been reported to confer high fosfomycin resistance when transformed into a fosfomycin-susceptible *E. coli* strain (Kumar *et al.*, 2009). Interestingly, this ortholog contains the conserved mobile-loop cysteine (Cys116 in VfiMurA) and shares high sequence identity with fosfomycin-susceptible MurA enzymes. In order to further understand additional intrinsic fosfomycin-resistance mechanisms, we have determined the crystal structure of MurA from *V. fischeri* in the presence of the substrate UNAG and fosfomycin at a resolution of 1.93 Å. We now report the preparation of an efficient recombinant protein-production system, crystallization, structure determination and comparisons with previously determined MurA structures.

2. Methods and materials

2.1. Cloning, expression and purification

The gene encoding VfiMurA for this study was PCR-amplified from *V. fischeri* MJ11 (ATCC No. BAA-1741) using the primers 5′-CCA ACC ATG GAT AAG TTT CGA ATT CAA GGA AGT GA-3′ and 5′-CCA ACT CGA GTA AGT CGT CGC TAT GAA CTC GCT CA-3′. The resulting PCR product incorporated *Nco*I and *Xho*I restriction sites and was ligated into the expression vector pET28a (Novagen). The ligation was transformed into chemically competent *E. coli* Top10 cells (Invitrogen) for plasmid amplification. A sequence-verified clone was then transformed into *E. coli* BL21 Star (DE3) (Invitrogen) for protein expression. The cloned open reading frame contained a C-terminal His_6 affinity tag.

The cells were grown at 310 K in 1 l Terrific Broth and were induced with 1 m*M* IPTG when the OD_{600} reached 0.8. The cells were harvested after an additional 12 h of growth at 291 K. Sonication was used to lyse the cells and the lysate was cleared by centrifugation. The supernatant was loaded onto a bed of Ni–NTA agarose and was eluted with a stepwise gradient of imidazole in 50 m*M* Tris, 200 m*M* NaCl pH 8.0. The final purification step was a size-exclusion column (Superdex 75 from GE Healthcare) previously equilibrated with buffer consisting of 25 m*M* Tris, 100 m*M* NaCl pH 8.0. The VfiMurA protein was soluble when overexpressed and was purified to >98% purity (as determined by SDS–PAGE).

2.2. Crystallization and X-ray data collection

The VfiMurA protein was prepared for crystallization trials by centrifugal concentration to 10 mg ml^{-1} followed by the addition of 5 m*M* UNAG and 2 m*M* fosfomycin from 100 m*M* aqueous stocks. Crystallization experiments were performed by the sitting-drop vapor-diffusion method using the following commercially available screens: The Classics II Suite and The PEGs and PEGs II Suites (Qiagen). 300 nl protein solution was mixed with 300 nl reservoir solution and duplicate plates were incubated at 277 and 298 K. The 298 K plates yielded overnight crystals in ∼20% of the drops and a similar observation was noted for the 277 K plates on day 2. A crystal grown at 277 K in 25%(*w*/*v*) PEG 3350, 0.1 *M* bis-tris pH 6.5 was cryoprotected in a solution consisting of 30% glycerol in mother liquor. Data were collected from one crystal on the MBC 4.2.2 beamline at the Advanced Light Source, Lawrence Berkeley National Laboratory using a wavelength of 1 Å, a sample-to-detector distance of 120 mm and an oscillation angle of 0.5°. A complete data set was recorded on a NOIR-1 CCD detector. Diffraction data were processed and scaled using *d*TREK*. The crystal belonged to space group $P2_1$ and contained four monomers in the asymmetric unit, with a solvent content of 43%. The unit-cell parameters and data-collection statistics are given in Table 1.

Table 1
Data-collection and refinement statistics for the MurA–UNAG–fosfomycin complex (PDB entry 3vcy).

Values in parentheses are for the highest resolution shell.

Data collection	
Space group	$P2_1$
Unit-cell parameters (Å)	a = 86.60, b = 118.51, c = 92.51
Resolution (Å)	1.93 (2.03–1.93)
No. of reflections	408188
No. of averaged (unique) reflections	122583
R_{merge} (%)	12.6 (47.1)
$\langle I/\sigma(I)\rangle$	4.8 (2.2)
Completeness (%)	97.2 (89.7)
Refinement	
Resolution range (Å)	27.9–1.93 (1.98–1.93)
No. of reflections	126033
No. of reflections in test set	6151
Completeness (%)	97 (87.7)
R_{cryst} (%)	19.9 (33.9)
R_{free} (%)	26.1 (37.3)
Wilson B factor (Å^2)	18.2
Average B factor (protein) (Å^2)	25.5
No. of protein molecules in asymmetric unit	4
R.m.s.d. from ideal geometry	
Bond lengths (Å)	0.009
Bond angles (°)	1.482
Ramachandran plot statistics	
Allowed (%)	98.4
Generously allowed (%)	1.5
Disallowed (%)	0.1

2.3. Structure solution and refinement

The structure of VfiMurA in complex with UNAG and fosfomycin was solved by molecular replacement with *Phaser* (McCoy *et al.*, 2007) in the *CCP*4 program suite (Winn *et al.*, 2011) using the coordinates of a single chain of *E. cloacae* MurA (PDB entry 3lth; Han *et al.*, 2010) as a search model. Refinement was carried out using *REFMAC*5.5 (Murshudov *et al.*, 2011; Mooij *et al.*, 2009). A total of 5% of the data were kept aside for R_{free} calculations. After a few rounds of restrained refinement, significant electron density was observed in the active site for UNAG and fosfomycin as well as a phosphate ion and a glycerol molecule. Model building and incorporation of solvent and ligands were performed with the program *Coot* (Emsley *et al.*, 2010). The final refinement and geometry statistics are provided in Table 1. The final model has an R_{cryst} of 19.9%, an R_{free} of 26.1% and a mean figure of merit (FOM) of 0.83. The model was validated using *PROCHECK* (Laskowski *et al.*, 1993) and *RAMPAGE* (Lovell *et al.*, 2003). The majority of the residues lie in the most favored and generously allowed regions of the Ramachandran plot (98.4 and 1.5%, respectively); however, two residues (0.1%) fell into the outlier region. These residues, Asn68 from chains *B* and *D*, are in a tight solvent-exposed turn between two β-sheets. The orientations of the main-chain and side-chain atoms in the outlier residues were clearly visible in electron density and facilitated the formation of networks of hydrogen bonds between atoms on opposite sides of the turn. The coordinates and structure factors of the structure of VfiMurA

complexed with UNAG and fosfomycin have been deposited in the Protein Data Bank with accession code 3vcy.

3. Results and discussion

3.1. Structure of VfiMurA

The enzyme comprises 429 amino acids, including a C-terminal hexahistidine tag, and has a molecular weight of 45 640 Da. The asymmetric unit in the crystal structure of VfiMurA contains four monomers with an average root-mean-square-difference (r.m.s.d.) between them of 0.26 Å (all-atom alignment), indicating that they are nearly identical structures (Fig. 1). There was no observed electron density for the C-terminal affinity tag or for the last three amino acids of the native sequence. The orientation of the fosfomycin in the four protein chains, while unambiguous in each monomer, is slightly different distal to the cysteine S atom (Fig. 2). This would indicate that fosfomycin in the half-open loop form is tolerated in several low-energy conformations and may not strongly influence the overall conformation of the mobile loop.

The VfiMurA structure has a highly similar overall fold to other known MurA structures. This is not surprising given the high sequence conservation and the essential function that the enzyme serves in peptidoglycan biosynthesis. VfiMurA shares highest sequence identity with the following structurally characterized othologs: *E. coli*, 79.8% identity (93.8% similar); *E. cloacae*, 79.8% identity (93.3% similar); *H. influenzae*, 70.2% identity (89.4% similar). Overlays indicate that our structure is most similar to the *H. influenzae* (HinMurA) ternary structure (PDB entry 2rl2; Yoon *et al.*, 2008) with regard to the mobile Cys-containing loop, which adopts the half-open conformation in both structures. The *E. coli* ternary structure (PDB entry 1uae; Skarzynski *et al.*, 1996) exhibits the closed-loop form in which the Cys–fosfomycin adduct is positioned deep in the active site in the putative PEP-binding site. In contrast, the unliganded *E. coli* structure places the mobile loop in an open conformation. A half-open conformation is also seen in the *E. cloacae* MurA product complex (PDB entry 1ryw; Eschenburg *et al.*, 2005).

Structural overlays of all of the structures with the half-open loop conformation suggest that the active-site loop (Pro113–Pro122) is occluded from adopting the closed form by a tightly bound phosphate anion (or sulfate as modeled in HinMurA). In the case of VfiMurA the phosphate was carried throughout purification of the protein and could be detected in heat-denatured protein samples using the EnzChek Phosphate Assay Kit (Molecular Probes). It was not determined whether the presence of UNAG in the structure was a consequence of exogenous addition during crystallization or whether the protein sequestered the molecule during expression in the *E. coli* cytosol. Additionally, both the *E. cloacae* MurA (EclMurA) product complex (PDB entry 1ryw) and the VfiMurA complex have a glycerol molecule bound in close proximity to the phosphate that was introduced during cryoprotection of the crystal (Eschenburg *et al.*, 2005). Our study revealed that fosfomycin binds to VfiMurA in a manner

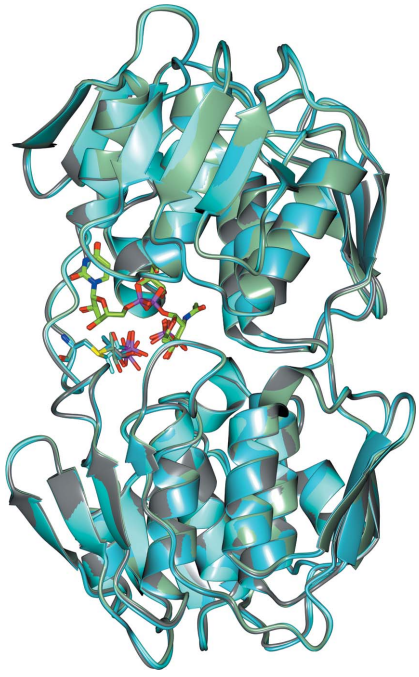

Figure 1
Structural overlay of the four monomers found in the crystallographic asymmetric unit. The structures are similar, with an average r.m.s.d. of 0.26 Å. UNAG, phosphate and glycerol (C atoms in green) from each chain are shown in the active-site pocket. The cysteine-bound fosfomycin from each protein chain is shown on the left side of the figure.

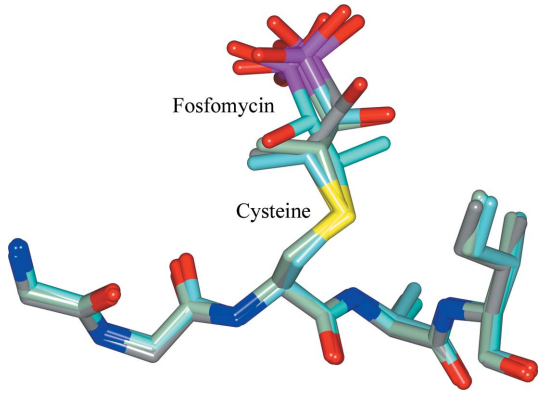

Figure 2
The orientation of the cysteine–fosfomycin adduct was variable in the four protein chains. The relative conformations of the adducts in the four monomers are shown together with two residues on either side.

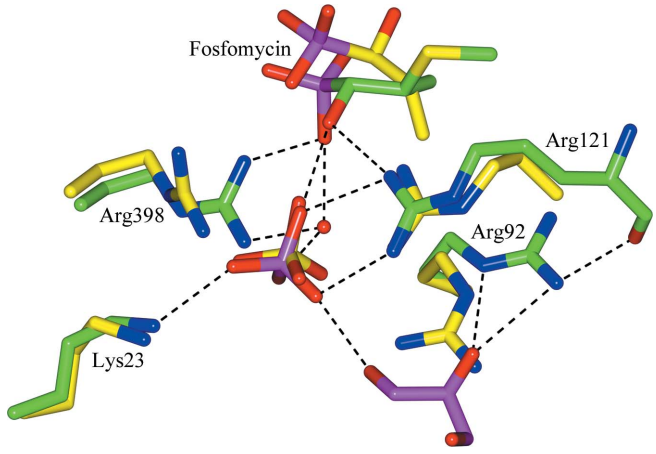

Figure 3
Comparison of the anion-binding sites of VfiMurA (green C atoms) and HinMurA (yellow C atoms). Potential hydrogen bonds are shown as dotted lines. The bound phosphate and glycerol are coordinated by Lys23, Arg92, Arg121 and Arg398. The HinMurA structure does not contain a glycerol molecule near the active site, allowing Arg92 of HinMurA to adopt a conformation in which it hydrogen bonds to the anion. In chain *A* of VfiMurA fosfomycin is oriented such that it disrupts a direct hydrogen bond to the anion. The glycerol molecule forms two hydrogen bonds to the β-phosphate of UNAG (not shown). Hydrogen bonding to Arg121 and Lys23 is conserved in both structures.

similar to other bacterial orthologs, which contradicts prior microbiological data suggesting that VfiMurA is naturally fosfomycin-insensitive. Given the structural similarity to fosfomycin-susceptible MurA orthologs as well as the unambiguous formation of the cysteine adduct, we did not perform further biochemical analysis to determine the kinetics of inhibition of this enzyme by fosfomycin.

One key difference when comparing the HinMurA and VfiMurA structures is the lack of the observed glycerol molecule near the bound anion. The resulting side-chain movements highlight the different relative plasticities in the residues surrounding these ligands (Fig. 3). The presence of the anion and neighboring glycerol molecule in both the EclMurA and VfiMurA structures presents an interesting opportunity for the structure-based design of new small-molecule inhibitors of MurA. In both structures there is no apparent exit for UNAG (or EP-UNAG in the product complex) while the phosphate is bound. The product structure represents the moment prior to reopening of the mobile loop (Eschenburg *et al.*, 2005). A chemical series simultaneously capturing the hydrogen bonds made by both the anion and glycerol molecule could generate significant enzymatic potency and lead to the design of new inhibitor classes. The activity of new small molecules targeting this binding site could be synergistic with fosfomycin because the mobile loop would be forced into the open or half-closed conformation, which would free the cysteine for alkylation.

In summary, the crystal structure of MurA from the marine Gram-negative bacterium *V. fischeri* in complex with UNAG and the drug fosfomycin complements the existing body of structural data by highlighting the key active-site residues involved in product and substrate binding as well as reinforcing recent discoveries regarding the conformational changes in the mobile loop. Because VfiMurA is a robust crystallizer and shares a high degree of sequence identity to clinically relevant Gram-negative pathogens, the protein would be an ideal system for the structure-based drug design of novel MurA inhibitors.

References

Bugg, T. D. & Walsh, C. T. (1992). *Nat. Prod. Rep.* **9**, 199–215.

De Smet, K. A., Kempsell, K. E., Gallagher, A., Duncan, K. & Young, D. B. (1999). *Microbiology*, **11**, 3177–3185.

Emsley, P., Lohkamp, B., Scott, W. G. & Cowtan, K. (2010). *Acta Cryst.* D**66**, 486–501.

Eschenburg, S., Priestman, M. & Schönbrunn, E. (2005). *J. Biol. Chem.* **280**, 3757–3763.

Fillgrove, K. L., Pakhomova, S., Newcomer, M. E. & Armstrong, R. N. (2003). *J. Am. Chem. Soc.* **125**, 15730–15731.

Han, H., Yang, Y., Olesen, S. H., Becker, A., Betzi, S. & Schönbrunn, E. (2010). *Biochemistry*, **19**, 4276–4282.

Kahan, F. M., Kahan, J. S., Cassidy, P. J. & Kropp, H. (1974). *Ann. N. Y. Acad. Sci.* **235**, 364–386.

Kumar, S., Parvathi, A., Hernandez, R. L., Cadle, K. M. & Varela, M. F. (2009). *Arch. Microbiol.* **191**, 425–429.

Laskowski, R. A., MacArthur, M. W., Moss, D. S. & Thornton, J. M. (1993). *J. Appl. Cryst.* **26**, 283–291.

Lovell, S. C., Davis, I. W., Arendall, W. B. III, de Bakker, P. I., Word, J. M., Prisant, M. G., Richardson, J. S. & Richardson, D. C. (2003). *Proteins*, **50**, 437–450.

McCoy, A. J., Grosse-Kunstleve, R. W., Adams, P. D., Winn, M. D., Storoni, L. C. & Read, R. J. (2007). *J. Appl. Cryst.* **40**, 658–674.

McCoy, A. J., Sandlin, R. C. & Maurelli, A. T. (2003). *J. Bacteriol.* **185**, 1218–1228.

Mooij, W. T., Cohen, S. X., Joosten, K., Murshudov, G. N. & Perrakis, A. (2009). *Structure*, **17**, 183–189.

Murshudov, G. N., Skubák, P., Lebedev, A. A., Pannu, N. S., Steiner, R. A., Nicholls, R. A., Winn, M. D., Long, F. & Vagin, A. A. (2011). *Acta Cryst.* D**67**, 355–367.

Rigsby, R. E., Fillgrove, K. L., Beihoffer, L. A. & Armstrong, R. N. (2005). *Methods Enzymol.* **401**, 367–379.

Schönbrunn, E., Sack, S., Eschenburg, S., Perrakis, A., Krekel, F., Amrhein, N. & Mandelkow, E. (1996). *Structure*, **4**, 1065–1075.

Skarzynski, T., Mistry, A., Wonacott, A., Hutchinson, S. E., Kelly, V. A. & Duncan, K. (1996). *Structure*, **4**, 1465–1474.

Walsh, C. T., Benson, T. E., Kim, D. H. & Lees, W. J. (1996). *Chem. Biol.* **3**, 83–91.

Winn, M. D. *et al.* (2011). *Acta Cryst.* D**67**, 235–242.

Yoon, H.-J., Lee, S. J., Mikami, B., Park, H.-J., Yoo, J. & Suh, S. W. (2008). *Proteins*, **71**, 1032–1037.